Available online at www.sciencedirect.com
ScienceDirect
Journal of Photochemistry and Photobiology A: Chemistry 189 (2007) 295–300
Journal of Photochemistry and Photobiology A:Chemistry
www.elsevier.com/locate/jphotochem

Tetrahydroquinoline dyes with different spacers for organic dye-sensitized solar cells

Ruikui Chen [a], Xichuan Yang [a,*], Haining Tian [a], Licheng Sun [a,b,**]

[a] *State Key Laboratory of Fine Chemicals, DUT-KTH Joint Education and Research Center on Molecular Devices, Dalian University of Technology (DUT), Zhongshan Road 158-46, 116012 Dalian, PR China*

[b] *Center of Molecular Devices, Department of Chemistry, Organic Chemistry, Royal Institute of Technology (KTH), Teknikringen 30, 10044 Stockholm, Sweden*

Received 23 October 2006; received in revised form 25 January 2007; accepted 20 February 2007
Available online 23 February 2007

Abstract

Novel organic dyes (**C1-1**, **C1-5** and **C2-1**) with a tetrahydroquinoline moiety as the electron donor, different thiophene-containing electron spacers and a cyanoacrylic acid moiety as the electron acceptor have been designed and synthesized for the application in dye-sensitized solar cells (DSSCs). An interesting relationship between the dye structures, properties, and the performance of DSSCs based on these tetrahydroquinoline dyes is obtained. Although **C2-1** dye, which has a rigid electron spacer, has the narrowest action spectrum among these dyes, it gives the highest solar-to-electricity conversion efficiency (η) of 4.49% (V_{oc} = 600 mV, J_{sc} = 11.20 mA/cm^2, ff = 0.67) of a DSSC under simulated AM 1.5 irradiation (100 mW/cm^2). Under the same conditions, the η value of a DSSC based on N3 dye is 6.16%.

Keywords: Dye-sensitized solar cell; Sensitizer; Tetrahydroquinoline; Thiophene

1. Introduction

Dye-sensitized solar cells (DSSCs) have become one of the most promising low-cost alternatives for the photovoltaic conversion of solar energy compared with the conventional solid p–n junction photovoltaic devices [1,2]. The heart of a DSSC system is a mesoporous oxide layer composed of nanometer-sized particles anchored by a monolayer of the charge transfer dye such as Ru-polypyridyl-complex [2]. The most widely used sensitizer for the DSSCs application is *cis*-di-(thiocyanato)bis(4,4′-dicarboxy-2,2′-bipyridine) ruthenium(II), coded as N3 or N719 dye depending on whether it contains four or two protons [3,4]. High performance and good stability of DSSCs based on Ru dyes had been obtained in the literatures [5]. However, the Ru dyes are facing the problem of costs and environmental issues.

Metal-free dyes, which have many advantages such as large absorption coefficients (attributed to an intramolecular π–π^* transition), easily molecular design for desired photophysical and photochemical properties, inexpensive and environment friendly [6e,6g], are also adopted as sensitizers for DSSCs. But the efficiencies of DSSCs based on metal-free dyes are much lower than that of Ru dyes based solar cells. Recently, DSSCs performance based on metal-free organic dyes has been remarkably improved by several groups [6–14]. A much higher solar-to-electric power conversion efficiency of up to 9% in full sunlight has been achieved by Ito et al. using an indoline dye [14]. This result suggest that smart designed metal-free organic dyes are also highly competitive candidates for solar cells due to their low costs and easy synthesis.

Some electron donor acceptor π-conjugated (D-π-A) compounds have been found to possess photoinduced intramolecular charge transfer (PICT) properties [15]. The PICT character makes these compounds ideal dyes for DSSCs application. The charge transfer or separation between the electron donor and acceptor moieties in the molecule may facilitate the rapid electron injection from the dye molecule into the conduction band of the wide band semiconductor, e.g., TiO_2, which is required for efficient DSSCs. The cations formed after the electron injection are also in good match to the redox of the common used elec-

* Corresponding author. Tel.: +86 411 88993886; fax: +86 411 83702185.
** Corresponding author at: Center of Molecular Devices, Department of Chemistry, Organic Chemistry, Royal Institute of Technology (KTH), Teknikringen 30, 10044 Stockholm, Sweden. Tel.: +46 8 7908127; fax: +46 8 7912333.
E-mail addresses: yangxc@dlut.edu.cn (X. Yang), lichengs@kth.se (L. Sun).

1010-6030/$ – see front matter © 2007 Elsevier B.V. All rights reserved.
doi:10.1016/j.jphotochem.2007.02.018

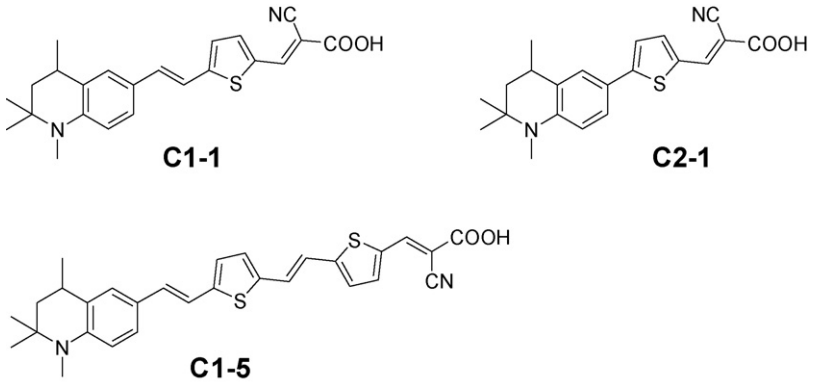

Fig. 1. Chemical structures of the tetrahydroquinoline dyes.

trolyte, I^-/I_3^-. In this paper, we report the design, synthesis and characterization of a series of organic dyes of this type aimed at providing a better understanding of the relationship between dye structures and performance of the DSSCs. The structures of these dyes are shown in Fig. 1. The same electron donor of 1,2,2,4-tetramethyl-1,2,3,4-tetrahydroquinoline, and the same electron acceptor, cyanoacrylic acid group are used in all these three dyes. However, different types of spacers containing thiophene moiety are adopted to the π-conjugating backbone for adjusting the absorption spectra, HOMO and LUMO levels of the dyes. Our results show that even a small change in the spacer of the dye can cause a significant change in the solar cell performance.

2. Experimental details

2.1. Synthesis

The synthesis of the dyes was carried out under classical procedures and is shown in Scheme 1. The electron donor, 1,2,2,4-tetramethyl-1,2,3,4-tetrahydroquinoline (**1**), was synthesized using improved literature procedures and served as starting compound [16,17]. The synthetic details will be published elsewhere. The characterization data of these dyes are listed below.

2-Cyano-3-{5-[2-(1,2,2,4-tetramethyl-1,2,3,4-tetrahydroquinolin-6-yl)-vinyl]-thiophen-2-yl}-acrylic acid (**C1-1**). Black solid (yield 80%). Mp: 208–210 °C. ^{1}H NMR (DMSO-d_6, 400 MHz, ppm): δ 1.17 (s, 3H), 1.27 (s, 3H), 1.33 (d, J = 6.6 Hz, 3H), 1.41 (dd, J_1 = 12.6 Hz, J_2 = 12.9 Hz, 1H), 1.83 (dd, J_1 = 4.2 Hz, J_2 = 13.0 Hz, 1H), 2.77–2.80 (m, 4H), 6.54 (d, J = 8.7 Hz, 1H), 7.00 (d, J = 16.1 Hz, 1H), 7.18 (d, J = 3.9 Hz, 1H), 7.21 (d, J = 16.0 Hz, 1H), 7.30 (d, J = 8.5 Hz, 1H), 7.34 (s, 1H), 7.59 (d, J = 3.9 Hz, 1H), 8.06 (s, 1H). HRMS-EI (*m/z*): $[M\text{-}CO_2]^+$ calcd for $C_{22}H_{24}N_2S$, 348.1660; found, 348.1656.

2-Cyano-3-[5-(2-{5-[2-(1,2,2,4-tetramethyl-1,2,3,4-tetrahydro-quinolin-6-yl)-vinyl]-thiophen-2-yl}-vinyl)-thiophen-2-yl]-acrylic acid (**C1-5**). Black solid (yield 64%). Mp: >260 °C. ^{1}H NMR (DMSO-d_6, 400 MHz, ppm): δ 1.17 (s, 3H), 1.26 (s, 3H), 1.33 (d, J = 6.6 Hz, 3H), 1.41 (dd, J_1 = 12.8 Hz, J_2 = 13.4 Hz, 1H), 1.83 (dd, J_1 = 4.1 Hz, J_2 = 12.8 Hz, 1H), 2.79 (m, 4H), 6.53 (d, J = 9.0 Hz, 1H), 6.84 (d, J = 16.3 Hz, 1H), 7.04 (d, J = 3.5 Hz, 1H), 7.09–7.17 (m, 2H), 7.23–7.35 (m, 5H), 7.75 (s, 1H), 8.20 (s, 1H). HRMS-EI (*m/z*): $[M\text{-}CO_2]^+$ calcd for $C_{28}H_{28}N_2S_2$, 456.1694; found, 456.1693.

2-Cyano-3-[5-(1,2,2,4-tetramethyl-1,2,3,4-tetrahydro-quinolin-6-yl)-thiophen-2-yl]-acrylic acid (**C2-1**). Red brown solid (yield 83%). Mp: 185–190 °C. ^{1}H NMR (DMSO-d_6, 400 MHz, ppm): δ 1.19 (s, 3H), 1.29 (s, 3H), 1.34 (d, J = 6.5 Hz, 3H), 1.43 (dd, J_1 = 12.4 Hz, J_2 = 13.3 Hz, 1H), 1.86 (dd, J_1 = 4.2 Hz, J_2 = 13.0 Hz, 1H), 2.82–2.84 (m, 4H), 6.61 (d, J = 8.4 Hz, 1H), 7.42–7.45 (m, 2H), 7.49 (d, J = 3.7 Hz, 1H), 7.82 (d, J = 3.6 Hz, 1H), 8.27 (s, 1H). HRMS-EI (*m/z*): $[M\text{-}CO_2]^+$ calcd for $C_{20}H_{22}N_2S$, 322.1504; found, 322.1498.

2.2. Analytical measurements

The absorption and emission spectra were measured on a HP-8453 spectrophotometer and PTI-C-700 fluorescence spectrometer, respectively. The ^{1}H NMR spectra were recorded on a VARIAN INOVA 400 MHz NMR spectrometer. High resolution mass spectral determinations were made on a Micromass GC-Tof MS instrument. Melting-points were measured with a X-4 melting-point apparatus with microscope. Electrochemical redox potentials were obtained by cyclic voltammetry using a three-electrode cell and an electrochemistry workstation (BAS100B, USA). The working electrode was a glass carbon electrode; the auxiliary electrode was a Pt wire and Ag/Ag^+ was used as reference electrode. Tetrabutylammonium hexaflourophosphate ($TBAPF_6$, 0.1 M) was used as supporting electrolyte in DMF. Ferrocene was added to each sample solution at the end of the experiments and the ferrocenium/ferrocene (Fc/Fc^+) redox couple was used as an internal potential reference. The potentials versus NHE are calibrated by addition of 630 mV to the potentials versus Fc/Fc^+ [11].

2.3. Fabrication of the nanocrystalline TiO_2 solar cells

Titania paste was prepared from P25 (Degussa, Germany) following literature procedure [3] and deposited onto the F-doped tin oxide conducting glass (TEC8, sheet resistance of 8 Ω/square, Pilkington, USA) by doctor-blading. The resulted layer photoelelctrode of 10 μm thickness, was sintered at 500 °C for 30 min in air. The sintered film was further treated with

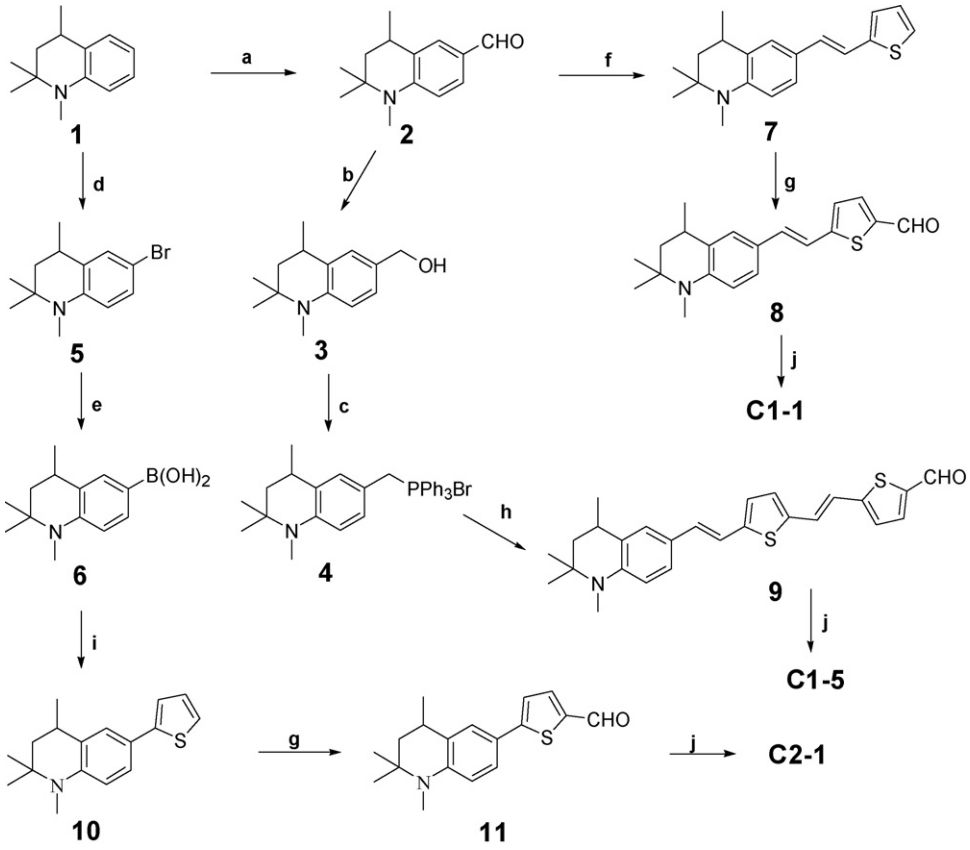

Scheme 1. Synthesis routes of the dyes. (a) DMF/$POCl_3$, 55 °C, 6 h, 55%; (b) $NaBH_4$, alcohol, r.t. 2 h, 99%; (c) PPh_3HBr, $CHCl_3$, reflux for 3 h, 37%; (d) NBS, CCl_4, r.t. 2 h, 93%; (e) (i) *n*-BuLi, THF, −78 °C, 1 h; (ii) $B(OBu)_3$, −78 °C to r.t., overnight; (iii) 2% HCl, 68%; (f) diethyl 2-thienylmethylphosphonate, *t*-BuOK, THF, 0 °C, 2 h, 95%; (g) (i) *n*-BuLi, THF, −15 °C, 20 min; (ii) DMF, −15 °C, 2 h; (iii) water; (h) *E*-1,2-Bis(2-formyl-5-thienyl)ethene, K_2CO_3, DMF, 18-crown-6-ether, r.t. 2 h, 54%; (i) 2-thienylboronic acid, K_2CO_3, $Pd(PPh_3)_4$, 1,2-dimethoxy-ethane, reflux for 8 h. 85%; (j) cyano-acetic acid, CH_3CN, piperidine, reflux for 2 h.

40 mM $TiCl_4$ aqueous solution at 70 °C for 30 min, then washed with water and ethanol, and annealed at 500 °C for 30 min. After the film was cooled to 80 °C, it was immersed into a 2×10^{-4} M dye solution in ethanol and maintained under dark overnight. The electrode was then rinsed with ethanol and dried. One drop of electrolyte solution was deposited onto the surface of the electrode and penetrated inside the TiO_2 film via capillary action. The electrolyte consisted of 0.6 M 1,2-dimethyl-3-propylimidazolinium iodine (DMPII), 0.1 M LiI, 0.05 M I_2 and 0.5 M 4-*tert*-butylpyridine (TBP) in 3-methoxypropionitrile. A platinized counter electrode was then clipped onto the top of the TiO_2 working electrode to form our test cell.

2.4. Photocurrent–voltage measurements

The irradiation source for the photocurrent density–voltage (*J–V*) measurement is an AM 1.5 solar simulator (16S-002, SolarLight Co. Ltd., USA). The incident light intensity was 100 mW/cm^2 calibrated with a standard Si solar cell. The tested solar cells were masked to a working area of 0.159 cm^2. The current–voltage curves were obtained by linear sweep voltammetry (LSV) method using an electrochemical workstation (LK9805, Lanlike Co. Ltd., China). The incident photon-to-current conversion efficiency (IPCE) was measured with a Hypermonolight (SM-25, Jasco Co. Ltd., Japan).

3. Results and discussion

The absorption spectra of these three dyes in ethanol solution and on the TiO_2 electrode film are shown in Fig. 2. The corresponding photophysical data are collected in Table 1. It can be found from Fig. 2 that the absorption properties of the dyes are affected by the electron spacers greatly. The absorption spectra are red-shifted and expanded when the thienylvinyl electron spacer is introduced to the dye molecules (**C1-1** and **C1-5** dyes), compared with **C2-1** dye which contains only one thienyl group as the spacer. The absorption spectra of these dyes on TiO_2 film are broadened and blue-shifted by 8, 70, and 4 nm for **C1-1**, **C1-5** and **C2-1**, respectively. Such phenomenon has been observed in other organic dyes [6g]. The reason for the blue-shifts of absorption could be ascribed to the aggregation of the dyes on the surface of TiO_2. Particularly, **C1-5** dye has relatively larger blue-shift (70 nm) than the other two dyes, the two thienylvinyl moieties in the spacer of **C1-5** might be responsible for the stronger aggregation. This result also indicates that among these three dyes, **C2-1** is the most less aggregated one on the surface of TiO_2.

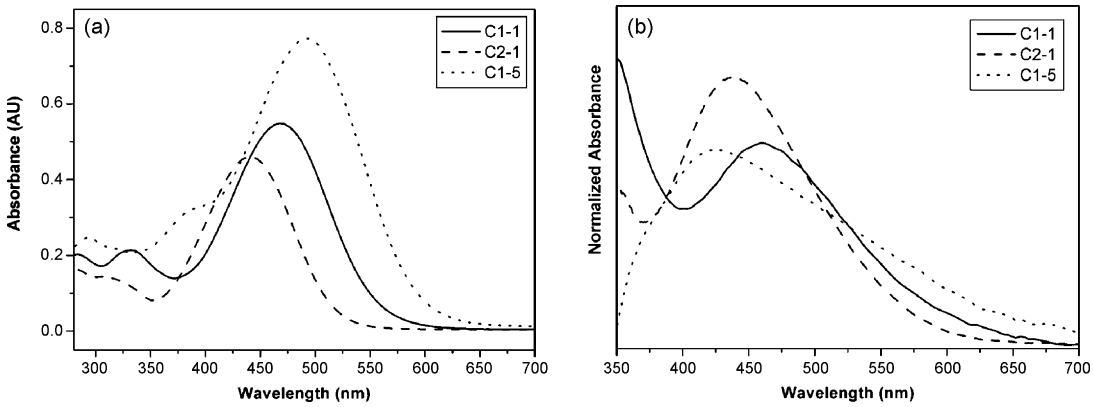

Fig. 2. (a) Absorption spectra of the dyes in ethanol solution (2×10^{-5} M) and (b) absorption spectra of the dyes adsorbed on a transparent TiO_2 film.

Table 1
The absorption, emission and electrochemical properties of the dyes

Dye	Absorption[a]			Emission[a]	E_{0-0} (V) (Abs/Em)[b]	E_{ox} (V vs. NHE)[c]	$E_{ox} - E_{0-0}$ (V vs. NHE)
	λ_{max} (nm)	ε at λ_{max} (M^{-1} cm^{-1})	λ_{max} on TiO_2 (nm)	λ_{max} (nm)			
C1-1	468	27,500	460	647	2.20	0.805	−1.395
C1-5	492	38,700	422	656	2.17	0.721	−1.449
C2-1	441	23,000	437	594	2.38	0.955	−1.425

[a] Absorption and emission spectra were measured in ethanol solution (2×10^{-5} M) at 25 °C.
[b] The zeroth–zeroth transition E_{0-0} value was estimated from the intersection of the absorption and emission spectra.
[c] Cyclic voltammetry of the oxidation behaviour of the dyes were measured in dry DMF containing 0.1 M tetrabutylammonium hexaflourophosphate ($TBAPF_6$) as supporting electrolyte (working electrode: glassy carbon; reference elelctrode: Ag/Ag^+ calibrated with Ferrocene/Ferrocenium (Fc/Fc^+) as an internal reference; counter electrode: Pt).

In order to get efficient charge separation, the HOMO and LUMO level of the dye must match with the conduction-band-edge energy level (E_{cb}) of the TiO_2 and the redox potential of electrolyte. The first oxidation potentials (E_{ox}) corresponding to the HOMO levels of the dyes were measured by cyclic voltammetry (CV) method in DMF solution. We consider that the potential levels of $E_{ox} - E_{0-0}$, where E_{0-0} is the zeroth–zeroth energy of the dyes estimated from the intersection of the absorption and emission spectra, correspond to the LUMO levels of the dyes. These data are also listed in Table 1. The HOMO levels of **C1-1**, **C1-5** and **C2-1** (0.805 V, 0.721 V, 0.955 V versus NHE, respectively) are sufficiently more positive than the iodide/triiodide redox potential value, indicating that the oxidized dyes formed after electron injection to TiO_2 could accept electrons from I^- ions thermodynamically. The LUMO levels of **C1-1**, **C1-5** and **C2-1** dyes are −1.395 V, −1.449 V, and −1.425 V versus NHE, respectively. These values are sufficiently more negative than the E_{cb} of the TiO_2 electrode, −0.5 V versus NHE [18]. The relatively large energy gaps between the LUMO levels and E_{cb} allows for the addition of 4-*tert*-butylpyridine to the electrolyte, which shifts the E_{cb} of the TiO_2 negatively and, consequently, improves the voltage and the total efficiency [6f].

Photovoltaic properties of the solar cells constructed from these organic dye-sensitized TiO_2 electrodes were measured. The open-circuit photovoltage (V_{oc}), short-circuit photocurrent density (J_{sc}), fill factor (ff), and solar-to-electricity conversion efficiencies (η) are listed in Table 2. The η values of the **C1-1**, **C1-5** and **C2-1** sensitized solar cells are 2.93%, 1.19%, and 4.47%, respectively. When chenodexoycholic acid (CDCA, 3×10^{-3} M) was added to the dye bath as a coadsorbent to prevent aggregation, much higher photovoltaic performances are achieved, especially for **C1-5** dye. The corresponding photovoltaic data are also collected in Table 2. The J_{sc} and η values for DSSCs based on **C1-5** dye before and after the addition of CDCA

Table 2
Photovoltaic performance of DSSCs based on pure dyes and dyes with chenodexoycholic acid (CDCA, 3×10^{-3} M) as coadsorbent, compare with the **N3** dye[a]

Dye	V_{oc} (mV)	J_{sc} (mA/cm^2)	Fill factor (ff)	η (%)
C1-1	582	7.80	0.65	2.93
C1-1 + CDCA	583	8.48	0.64	3.17
C1-5[b]	532	3.39	0.66	1.19
C1-5 + CDCA[b]	542	7.22	0.59	2.32
C2-1	600	11.3	0.66	4.47
C2-1 + CDCA	600	11.2	0.67	4.49
N3[c]	695	14.03	0.63	6.16

[a] TiO_2 electrode were sensitized in a ethanol solution (2×10^{-4} M), film thickness is 10 μm, working area is 0.159 cm^2, measured under AM 1.5 (100 mW/cm^2) irradiation.
[b] The concentration of **C1-5** dye is 1×10^{-4} M.
[c] The concentration of **N3** dye is 3×10^{-4} M in ethanol.

are 3.39 and 7.22 mA/cm^2, 1.19% and 2.32%, respectively, indicating a strong aggregation without the CDCA addition. The photocurrent voltage curves based on these dye-sensitized solar cells after the addition of CDCA to the dye bath are shown in Fig. 3. For the optimized result, the V_{oc} is 600 mV, J_{sc} is 11.20 mA/cm^2, ff is 0.67, and the η value is 4.49% for **C2-1** dye. When we measured the performance of a DSSC based on the N3 dye under the same conditions, the η value is 6.16%.

It is interesting to note that the η values are inverse proportional to the light absorption capabilities of the dyes. **C2-1** dye, which has the lowest light absorption capability, gives the highest η value compares with **C1-1** and **C1-5** dyes. This indicates that the elimination of the C=C double bond in the dye structure is useful for getting higher η value, although the C=C double bond can increase the light absorption ability. In a previous study [15], we found that the excited state of a similar molecule where the carboxylate group in **C1-1** is replaced by a phosphonate group, adopt a twisted intramolecular charge transfer geometry. We suggest that similar twisting processes will also happen in the **C1-1** and **C1-5** dyes which contain C=C double bond, leading to the possible *trans–cis* photoisomerization. These processes may decrease the excited state energy of these dyes and result in a less efficiency of electron injection.

The action spectra of the incident photon-to-current conversion efficiencies for DSSCs based on the tetrahydroquinoline dyes are shown in Fig. 4. The onset wavelength of the IPCE spectrum for DSSC based on **C2-1** dye is 700 nm. IPCE values higher than 70% are observed in the range of 430–540 nm with a maximum value of 79% at 460 nm for **C2-1** dye. When the reflection and absorption losses in the TCO substrate are considered, the net photon-to-current conversion efficiency in this range exceeds 90%, which indicates the highly efficient performance of these solar cells. The onset wavelengths of the IPCE spectra of DSSCs based on **C1-1** and **C1-5** dyes are 780 nm, but the highest IPCE values are 54% at 460 nm, 39% at 500 nm, respectively. The lower IPCE values result in the lower conversion efficiencies under white-light irradiation.

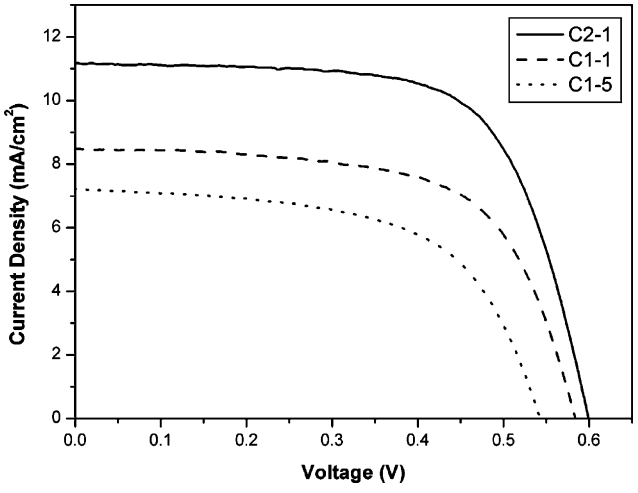

Fig. 3. Photocurrent voltage curves obtained with DSSCs based on tetrahydroquinoline dyes with the addition of CDCA (3×10^{-3} M) to the dye bath under AM1.5 irradiation (100 mW/cm^2).

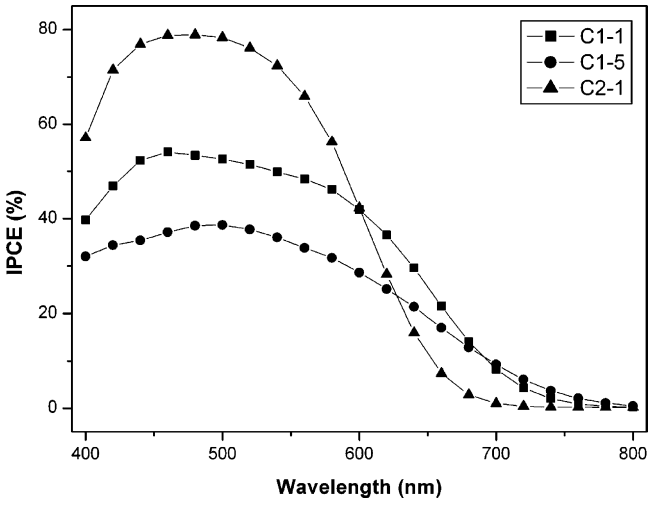

Fig. 4. Incident photon-to-current conversion efficiency spectra for DSSCs based on tetrahydroquinoline dyes.

The lower performance of the DSSCs based on the tetrahydroquinoline dyes is probably due to the narrow action spectra in the whole solar spectrum. For **C1-1** and **C1-5** dyes, the action spectra expand but the highest IPCE values decrease. A higher η value is obtained by the rigid **C2-1** dye, although the action spectrum is rather narrow. This indicates that dyes with rigid molecular structure should be paid much attention to improve the solar cell performance.

4. Conclusions

Three pure organic dyes, **C1-1**, **C1-5** and **C2-1**, have been designed and synthesized. These dyes have the same electron donor (tetrahydroquinoline) and acceptor (cyanoacrylic acid), but different conjugating linkage. The DSSCs performance based on these dyes provides different results. **C2-1** dye with a rigid linkage has a narrowest action spectrum, but gives the highest η value compares with the **C1-1** and **C1-5** dyes. A maximum η value of 4.49% has been obtained under simulated AM 1.5 irradiation (100 mW/cm^2) with a DSSC based on **C2-1** dye (V_{oc} = 600 mV, J_{sc} = 11.20 mA/cm^2, ff = 0.67), in comparison with 6.16% of N3 dye under the same conditions. Our results suggest that the dyes with rigid molecular structures are helpful for getting higher solar-to-electricity conversion efficiencies in DSSCs. For further dye sensitizer engineering, the rigid larger π-conjugating systems are expected for better light harvesting ability, and thus better performance of the dyes.

Acknowledgements

This work is supported by the Programme of Introducing Talents of Discipline to Universities. We thank the National Natural Science Foundation of China (Grant no. 20633020), the Ministry of Science and Technology (MOST), Ministry of Education (MOE), the Swedish Energy Agency, the K&A Wallenberg Foundation and the Swedish Research Council for financial support. The authors would also like to thank Prof.

Songyuan Dai at Institute of Plasma Physics, CAS, China for the kind help on solar cell test. We are also grateful to Dr. Hongguang Cui at DUT, Tannia Marinado and Daniel P. Hagberg at Royal Institute of Technology, Sweden for helpful discussion.

References

[1] M. Grätzel, Nature 414 (2001) 338–344.
[2] M. Grätzel, J. Photochem. Photobiol. A 164 (2004) 3–14.
[3] M.K. Nazeeruddin, A. Key, I. Rodicio, R. Humphry-Barker, E. Müller, P. Liska, N. Vlachopoulous, M. Grätzel, J. Am. Chem. Soc. 115 (1993) 6382–6390.
[4] M.K. Nazeeruddin, S.M. Zakeeruddin, R. Humphry-Baker, M. Jirousek, P. Liska, N. Vlachopoulos, V. Shklover, Christian-H. Fischer, M. Grätzel, Inorg. Chem. 38 (1999) 6298–6305.
[5] M. Grätzel, Inorg. Chem. 44 (2005) 6841–6851.
[6] (a) K. Hara, K. Sayama, Y. Ohga, A. Shinpo, S. Suga, H. Arakawa, Chem. Commun. (2001) 569–570;
(b) K. Hara, M. Kurashige, S. Ito, A. Shinpo, S. Suga, K. Sayama, H. Arakawa, Chem. Commun. (2003) 252–253;
(c) K. Hara, M. Kurashige, Y. Dan-oh, C. Kasada, A. Shinpo, S. Suga, K. Sayamaa, H. Arakawa, New J. Chem. 27 (2003) 783–785;
(d) K. Sayama, S. Tsukagoshi, K. Hara, Y. Ohga, A. Shinpou, Y. Abe, S. Suga, H. Arakawa, J. Phys. Chem. B 106 (2002) 1363–1371;
(e) K. Hara, Y. Tachibana, Y. Ohga, A. Shinpo, S. Sugab, K. Sayamaa, H. Sugiharaa, H. Arakawa, Sol. Energy Mater. Sol. Cells 77 (2003) 89–103;
(f) K. Hara, T. Sato, R. Katoh, A. Furube, T. Yoshihara, M. Murai, M. Kurashige, S. Ito, A. Shinpo, S. Suga, H. Arakawa, Adv. Funct. Mater. 15 (2005) 246–252;
(g) K. Hara, Z.-S. Wang, T. Sato, A. Furube, R. Katoh, H. Sugihara, Y. Dan-oh, C. Kasada, A. Shinpo, S. Suga, J. Phys. Chem. B 109 (2005) 15476–15482.
[7] (a) Z.-S. Wang, F.-Y. Li, C.-H. Huang, Chem. Commun. (2000) 2063–2064;
(b) Z.-S. Wang, F.-Y. Li, C.-H. Huang, J. Phys. Chem. B 105 (2001) 9210–9217.
[8] (a) T. Kitamura, M. Ikeda, K. Shigaki, T. Inoue, N.A. Anderson, X. Ai, T. Lian, S. Yanagida, Chem. Mater. 16 (2004) 1806–1812;
(b) S. Yanagida, G.K.R. Senadeera, K. Nakamura, T. Kitamura, Y. Wada, J. Photochem. Photobiol. A 166 (2004) 75–80.
[9] K.R. Justin Thomas, J.T. Lin, Y.C. Hsu, K.C. Ho, Chem. Commun. (2005) 4098–4100.
[10] S. Tan, J. Zhai, H. Fang, T. Jiu, J. Ge, Y. Li, L. Jiang, D. Zhu, Chem. Eur. J. 11 (2005) 6272–6276.
[11] D.P. Hagberg, T. Edvinsson, T. Marinado, G. Boschloo, A. Hagfeldt, L. Sun, Chem. Commun. (2006) 2245–2247.
[12] S.L. Li, K.J. Jiang, K.F. Shao, L.M. Yang, Chem. Commun. (2006) 2792–2794.
[13] (a) T. Horiuchi, H. Miura, S. Uchida, Chem. Commun. (2003) 3036–3037;
(b) T. Horiuchi, H. Miura, S. Uchida, J. Photochem. Photobiol. A 164 (2004) 29–32;
(c) T. Horiuchi, H. Miura, K. Sumioka, S. Uchida, J. Am. Chem. Soc. 126 (2004) 12218–12219.
[14] S. Ito, S.M. Zakeeruddin, R. Humphry-Baker, P. Liska, R. Charvet, P. Comte, M.K. Nazeeruddin, P. Péchy, M. Takata, H. Miura, S. Uchida, M. Grätzel, Adv. Mater. 18 (2006) 1202–1205.
[15] R. Chen, G. Zhao, X.Yang, X. Jiang, J. Liu, H. Tian, Y. Gao, K. Han, M. Sun, L. Sun, J. Mol. Struct., submitted for publication.
[16] D. Craig, J. Am. Chem. Soc. 60 (1938) 1458–1465.
[17] M.Yu. Krysin, Kh.S. Shikhaliev, I.K. Anokhina, Zh.V. Shmyreva, Chem. Heterocycl. Compd. 37 (2001) 227–230.
[18] A. Hagfeldt, M. Grätzel, Chem. Rev. 95 (1995) 49–68.